Research Square

Preprints are preliminary reports that have not undergone peer review. They should not be considered conclusive, used to inform clinical practice, or referenced by the media as validated information.

Non-linear correction method for Si photodiode detectors and its application to the electro-optical measurement for the PDLC film

Xiangshen Meng
Southwest University

Jian Li (aizhong@swu.edu.cn)
Southwest University https://orcid.org/0000-0002-6053-7892

Yueqiang Lin
Southwest University

Xiaodong Liu
Southwest University

Decai Li
Tsinghua University

Zhenghong He
Southwest University

Research Article

Keywords: photodiode, detector, polymer dispersed liquid crystal, electro-optical response

Posted Date: July 14th, 2022

DOI: https://doi.org/10.21203/rs.3.rs-1845990/v1

License: This work is licensed under a Creative Commons Attribution 4.0 International License.
Read Full License

Non-linear correction method for Si photodiode detectors and its application to the electro-optical measurement for the PDLC film

Xiangshen Meng[1,2], Jian Li[1], Yueqiang Lin[1], Xiaodong Liu[1], Decai Li[3*], Zhenghong He[1**]

[1] School of Physical and Technology, Southwest University, Chongqing, 400715, China

[2] School of Mechanical and Control Engineering, Beijing Jiaotong University, Beijing, 100044, China

[3] State Key Laboratory of Tribology, Tsinghua University, Beijing, 100084, China

*Corresponding author

Decai Li

e-mail: lidecai@stinghua.edu.cn

**Corresponding author

Zhenghong He

e-mail:hezhenho@swu.edu.cn

Abstract

A corrected measurement method based on the silicon photodiode detector was investigated. The silicon photodiode detector is a fast response, but the measured transmittance error between the light power meter occurs and depends on the incident light power. In our work, the non-linear empirical formula was derived from the measured results of the silicon photodiode detector and light power meter. In addition, the formula was used to correct the measuring results of the polymer dispersed liquid crystal, and the corrected results are identical to those of the light power meter. The experimental results further show that the silicon photodiode detector is faster than the light power meter when measuring electro-optical response. As a result, the corrected method is reliable.

Keywords: photodiode, detector, polymer dispersed liquid crystal, electro-optical response

1 Introduction

Optical measurement is required to meet optical requirements, such as optical communication, applied optical measurement, laser processing, and others. A photodetector is a device that measures optical power or photon flux by converting the energy of absorbed photons into a measurable form [1]. The two main photodetectors commonly used are thermoelectric detectors and photoelectrical detectors. Thermoelectric detectors convert photon energy to heat, which measures the total output across a wide range of wavelengths. Due to the time it takes to change temperature, thermoelectric detectors' sensitivity and temporal response are inadequate to measure a fast response. Photoelectrical detectors are based on the photoelectric effect, and the absorption of photons causes the transition of electrons to higher energy levers, resulting in movable load carriers. Under an applied electric field, these carriers move and produce a measurable electric current. Photoelectrical detectors are composed primarily of photoconductive and semiconductor photodiode detectors. Photoconductor detectors based on photoconductivity depend directly on the increase in the electric conductivity of the light-induced material. The semiconductor photodiode detector is a p-n junction structure, and photons absorb through the depletion layer producing electrons and holes, and both carriers are adrift in opposite directions. In addition, this transport process induces an electric current in the external circuit. Semiconductor photodiode detectors are generally faster than photoconductor detectors because the strong field in the depletion region gives a high velocity to the photogenerated carriers [1]. Furthermore, semiconductor photodiode detectors deliver a voltage proportional to the light intensity and are used for ultraviolet to near-infrared region detection [2-5]. Silicon (Si) photodiode detectors (SPDs) are used widely as semiconductor photodiode detectors [6-8].

A matrix of randomly dispersed anisotropic polymers with liquid crystal droplets was produced, known as polymer dispersed liquid crystals (PDLC) [9]. A PDLC film is used for an electro-optical device because it can be switched from an opaque "off-state" to a light transparent "on-state" [10]. Among the characteristic parameters of the electro-optical effect of PDLC film, the transmittances T_0 and T_{sat} correspond to the off-state and saturated on-state. In

addition, the threshold voltage V_{th} and the saturation V_{sat} are the applied voltage at 10% and 90% of the T_{sat}, respectively [11].

Non-linearity is a well-known phenomenon in SPDs, significantly impacting optical measurement [12]. Calibration or correction is a prerequisite for accurate measurements. For instance, an electric surrogate radiometer calibrated the light power meter (LPM) [13]. The electro-optical measurement of the PDLC can also be corrected using the appropriate calibration standards [6]. In the work presented, the empirical formula was derived from the measured SPD voltage and LPM power and can be used to perfectly correct the SPD measurement of the PDLC.

2. Experimental methods and principles

2.1 Measurement of the SPD voltage and LPM power

In order to obtain the relationship between the SPD voltage and LPM power, the θ-scanning method was used [14]. The measurement setup is indicated in Fig. 1. A light beam was emitted by a He-Ne laser (1) (λ = 632.8 nm, Melles Griot) with a maximum output power of 15 mW. Then the light beam passed through a vertical polarizer (2) (Thorlabs) and a quarter-wave plate (3) (QWP, Thorlabs) with the polarization direction of the polarizer (2) 45º towards the optical axis of the QWP (3). The light transmitted by the QWP (3) was circularly polarized light and continued to cross a vertically polarized polarizer (4) (Thorlabs), and the output was vertically polarized light. The output beam was routed through a rotating polarizer (5) (Thorlabs) within the LabVIEW program. The output beam power changed with the angle θ of the polarizer (5). Moreover, the output light power was maximum when the polarizer (5) was vertically polarized (θ = 90º or 270º). The measurements of the SPD voltage and LPM power are as follows.

When the output light from the polarizer (5) was incident on a photoelectric sensor (6) (PES) (PD300R-UV, Ophir) connected with the LPM (7) (Starlite meter, Ophir), the light was converted into a current. The current was then converted into a power value corresponding to the standard value and displayed on the LPM (7). Meanwhile, the power can be saved in a computer (10) with LabVIEW via a data acquisition card (DAC) (9). Accordingly, the power

evolution curve with the rotation angle θ of the polarizer (5) can be obtained (curve P-θ), i.e., the θ-scanning.

When the output light from the polarizer (5) was an incident on an SPD (8) (7ID230, universal type, Sevan), the light can be converted into a current. The current is then converted into a voltage by the DAC (9) using the linear coupling of the resistance. Thus, the voltage evolution curve with the rotation angle θ of the polarizer (5) can be obtained (curve V-θ).

The relation V - P can also be obtained from the curves V-θ and P-θ.

2.2 Measurement of electro-optic effect for the PDLC

The PDLC film was prepared as Ref [15], with the mass ratio of the liquid crystal to the polymer being 50:50. The measurement for the electro-optical effect for the PDLC is shown in Fig. 2. A light beam emitted from the He-Ne laser (λ = 632.8 nm, Melles Griot) (1) passed through a changeable attenuator (2) to obtain the light beam with a different power. The light power from the attenuator (2) was measured using the LPM (StarLite with PD300R-UV, Ophir). Then the light beam passed through a vertical polarizer (3) (Thorlabs) and a QWP (4) (Thorlabs) with the polarization direction of the polarizer (3) 45º towards the optical axis of the QWP (4). The circularly polarized output light with adjustable light intensity passed through a vertical polarizer (5). The vertically polarized output light crossed a spectroscope (6) with a splitting ratio of 45 to 55. One output light beam from the spectroscope (6) passed through a diaphragm (7) and the PDLC film (8), another diaphragm (9), and the SPD (10) or the PES (12) of the LPM (13). When the SPDs measured the output light from the PDLC film (8), the current from the SPD (10) was saved as voltage V_t by the DAC (14) connected to the computer (16). Another output light beam from the spectroscope (6) was an incident to another SPD (11) as the reference light beam. The incident light output on the PDLC film (8) and the SPD (11) can be identical by adjusting the diaphragm (7) and saved as V_0 by the DAC (14). Accordingly, the transmittance through the SPDs is $T^V=V_t/V_0$. These two optical channels can compensate for fluctuations in the emission of the He-Ne laser (1) [16]. When the LPM measured the output light from the PDLC film (8), the light output measured through the PES (12) of the LPM (13) and the DAC (14) was saved as P_t. The measured reference light power was saved as P_0. Accordingly, the

transmittance through the LPM is $T^{P}=P_t/P_0$.

The voltage applied to the PDLC film was a square wave voltage at a frequency of 1kHz controlled by a voltage amplifier (15) and QAC (14) with computer (16) at a distance of 20 cm from the PDLC film (8) to the SPD (11) or PES (12). The light beam was a normal incident on the PDLC film and parallel to the applied electric field. The 2mm diameter aperture (9) has been placed in front of the detector to limit the light beam. The electro-optical measurements were performed at room temperature, about 19 ºC.

3. Result and discussion

3.1 *V-P* characteristics

Fig. 3 shows the *P-θ* and *V-θ* curves, and Fig. 4 shows the evolution curve *V-P* which comes from Fig. 3, is non-linear. With logarithmic function fitting, we obtained

$$V = 0.037 \cdot \ln(127.29 \cdot P + 1) \quad (1)$$

where the *P* and *V* units are respectively microwatt (μW) and volt (V). The experimental and fitting curves overlap perfectly, moreover, when $V = 0$, $P = 0$, as shown in Fig. 4.

3.2 Calibration of the PDLC electro-optic properties measurement results.

Figs. 5(a) and (b) show the transmittance curves with the applied voltage (T-V_{appl}) of the PDLC. T^{V} and T^{P} are the transmittances measured by the SPDs (Fig. 5 (a) and LPM (Fig. 5 (b), respectively. The T^{V} and T^{P} increase with the applied voltage and reach the saturation transmittance T_{sat} when the applied voltage is sufficiently high. No PDLC film transmittance is 100% in Figs. 5(a) and (b). However, the T^{V}-V_{appl} and T^{P}-V_{appl} curves are different. Fig. 5(a) shows that the T_0 and T_{sat} on the T^{V}-V_{appl} curve increase monotonically with the incident light power increasing. Fig. 5(b) shows that the T_0 and T_{sat} on the T^{P}-V_{appl} curve are independent of the incident light power. In addition, on the T^{V}-V_{appl} curve, T_0 is above 10 % T_{sat}, and V_{th} cannot be obtained. The electro-optical parameters of the PDLC are listed in Tab. 1. From Tab. 1, the V_{sat} from the SPDs increases with the incident light power increasing, and T_0, T_{sat}, V_{th}, and V_{sat} from the LPM are independent of the incident light power.

Light modulation by PDLC results from light scattering or non-linear optical effects and is not due to absorption. Thus, PDLC modulation is feasible in applications involving higher

power laser sources [17, 18]. Light modulation by the non-linear optical effect is a competition between the electric field of a high-intensity laser and the applied field [19]. The He-Ne laser (1) is a low-power continuous laser that cannot induce a significant non-linear optical effect or a temperature effect that affects the PDLC electro-optical properties [20]. As a result, T_0 and T_{sat} should not vary with the light power. Furthermore, the T^P-V_{appl} curves are nearly consistent at different incident light power. Therefore, we conclude that the electro-optical parameters of the PDLC obtained by the SPDs are incorrect. Figs. 5(a) and (b) show the difference between T^V and T^P. It is concluded that the difference is because the measured SPD voltage is non-linear as a proportion of the incident light power of the PDLC.

From Eq. (1),

$$P = \left(e^{0.037^{-1}\cdot V} - 1\right)/127.29 \tag{2}$$

The light intensity I is the light power per unit area. The transmittance T is the ratio of the transmitted light intensity I_t to the incident light intensity I_0, and P_t and P_0 are the transmitted and incident light powers, respectively. According to Eq. (2), the transmittance

$$\begin{aligned} T^P &= \frac{I_t}{I_0} = \frac{P_t}{P_0} \\ &= \frac{e^{0.037^{-1}\cdot V_t - 1}}{e^{0.037^{-1}\cdot V_0 - 1}} \end{aligned} \tag{3}$$

V_t and V_0 correspond to the transmitted and incident voltages of the SPDs on the PDLC film. From Eq. (3), usually, $T^P \neq V_t/V_0$. However, when 0 < x <1, $e^x \simeq 1 + x$ (the first-order Taylor expansion), and if V_t and V_0 are small enough, accordingly $T^P \approx V_t/V_0$. When the incident light power increases, the difference between V_t/V_0 and P_t/P_0 increases.

From Eq. (1), the transmittance from the SPDs

$$\begin{aligned} T^V &= \frac{V_t}{V_0} = \frac{0.03734\cdot\ln(127.29\cdot P_t+1)}{0.03734\cdot\ln(127.29\cdot P_0+1)} \\ &= \frac{\ln(\mathrm{A}\cdot \mathrm{P}_t+1)}{\ln(\mathrm{A}\cdot \mathrm{P}_0+1)}, A = 127.29 \end{aligned} \tag{4}$$

from Eq. (4),

$$P_t = \frac{1}{A}\left(e^{\left(T^V\cdot ln(A\mathrm{P}_0+1)\right)} - 1\right) \tag{5}$$

The corrected transmittance can be further obtained from Eq. (5),

$$T^{V,c} = \frac{P_t}{P_0} = \frac{1}{AP_0}\left(e^{\left(T^V \cdot ln(AP_0+1)\right)} - 1\right) \quad (6)$$

where A=127.29. As a result, when the incident light power P_0 is constant, AP_0 and ln(AP_0+1) are constant.

Fig. 6 shows the corrected curves $T^{V,c}$- V_{appl} of Fig. 5(a) according to Eq. (6), and the results show that the corrected curves $T^{V,c}$- V_{appl} coincides with the curves T^P-V_{appl}.

For the PDLC, when the applied voltage is high enough, the transmittance is the maximum, and the measured voltage of the SPDs, $V_t \approx V_0$, from Eq. (6),

$$T_{max}^{V,c} = \frac{1}{AP_0}\left(e^{\left(ln(AP_0+1)\right)} - 1\right)$$

$$\approx 1 \quad (7)$$

When the applied voltage is zero, the transmittance is the minimum, i.e., $V_t \rightarrow 0$, from Eq. (6),

$$T_{min}^{V,c} \approx 0 \quad (8)$$

According to Eqs. (7) and (8), for an ideal PDLC film, the transmittance $T^{V,C}$ varies from 0 to 1, with an increase of the applied voltage. Due to the refraction index difference between the liquid crystal droplets and the polymer and the light absorption, the actual PDLC film transmittance varies with voltage in $T_{min} > 0$ and $T_{max} < 1$.

Response time, i.e., rise and decay time, corresponding to the applied voltage switched on and off, is usually defined as the optical response [9]. When V_{appl} = 33 Vrms and the incident power is 1100 μW for the LPM and SPD, the response curves of the PDLC are shown in Fig. 7, and t = 1000 ms and 2000 ms, corresponding to the applied voltage is switched on and off respectively. Fig. 7 shows that the curve T^P-t has a noticeable delay; however, the delay can be negligible for the curve T^V-t. Besides, the curve $T^{V,c}$-t is obtained, and the T_{min} and T_{max} are equal to those of the curve T^P-t. As a result, the SPD is faster and more accurate.

4. Conclusion

The measurement results of the Si photodiode detector are non-linear in proportion to the incident light power. The empirical formula was obtained from the transmittances from the Si photodiode detector and the light power meter (T^V and T^P). In our work, a correction method based on the Si photodiode detector was proposed, and the measurement results of the Si photodiode detector were corrected when measuring the electro-optical effect of the PDLC film.

The experimental results show that the corrected transmittance curves $T^{V\text{-}c}$-V_{app} are consistent with the T^{P}-V_{appl} curves measured by the light power meter. Besides, the electro-optic effect parameters T_0, T_{sat}, V_{th}, and V_{sat} are independent of the incident light power. The light power meter can be directly used as a photodetector to measure the electro-optical effect of the PDLC to exclude the non-linear effect of the Si photodiode detector [21, 22]. However, when measuring the optical response of the PDLC, the delay time of the light power meter is more than the Si photodiode detector. Therefore, the correction method is a potential application related to response time.

Acknowledgments

This work was supported by Fundamental Research Funds for the Central Universities (grant number 2021YJS143), Natural Science Foundation of Chongqing, China (grand number cstc2021jcjy-msxmX1136), Doctoral Foundation of Southwest University (grant number SWU115010), National Natural Science Foundation of China (grant number 51735006, U1837206, 51927810), and Beijing Municipal Natural Science Foundation (grant number 3182013).

Declaration of interests

The authors declare that they have no known competing financial interests or personal relationships that could have appeared to influence the work reported in this paper.

References

[1] B. E. A. Saleh, M. C. Teich, Fundamentals of Photonics, John Wiely & Sons, Inc., Pub Lication, 3th edi., 2007, pp 748-803.

[2] X. Commerinhes, P. Davidson, C. Bourgaux, and J. Livage, Orientation of Liquid-Crystalline Suspensions of Vanadium Pentoxide Ribbons by a Magnetic Field, Adv. Matter. 1997, 11: 900-903.

[3] F. Lei, J. Fisher, Characterization of photodiodes in UV and visible spectral region based on cryogenic radiometry, Metrogia, 1993, 30: 297-303.

[4] M. Tanabe, Evaluation of the non-linearly of silicon photodiodes for ultraviolet light detection, Opt. Laser Tech., 2021, 138: 106852 (5pp).

[5] M. Tanbe, Spectral supralinearity of silicon photodiodes with over-filled illumination in the near-infrared region, Appl. Opt., 2020, 59: 8038-8046.

[6] U. Maschke, X. Coqueret, M. Benmouna, Electro-optical Properties of Polymer-Dispersed Liquid Crystals, Macromol. Rapid Commun., 2002, 23: 159-170.

[7] Y. Zhang, L. Zhou, J. Yang, J. Zhang, M. Hai, L.Zhang, F, Li, C. Zhang, Z. Yang, H. Yang and S. Zhu, Effects of crosslinking agent/diluents/thiol on morphology of the polymer matrix and electro-optical properties of polymer-dispersed liquid crystal Liq. Cryst., 2018, 45: 728-735.

[8] G. N.Hassanein, N. Kattan, M. A.Ellabban, Electro-optic properties of aligned and non-aligned polymer dispersed liquid crystals driven by an amplitude-modulated electric signal, Optik, 2019, 186:137-146.

[9] S. Singh, J. K. Srivastava, and R. K. Singh, Polymer Dispersed Liquid Crystals. In: Liquid Crystalline Polymers, Edi. By V.K. Thakur, M.R. Keller, Springer Inter Pub Swithzerland; 2016. pp 195-250.

[10] N. A. Vaz, G. W. Smith and G. P. Montgomery Jr. A Light Control Film Composed of Liquid Crystal Droplets Dispersed in a UV-Curable Polymer, Liq. Cryst., 1987, 146: 1-15.

[11] L. Bouteiller and P. L. Barny, Polymer-dispersed liquid crystals: Preparation, operation and application, Liq. Cryst., 1996, 21: 157-174.

[12] T. Kübarsepp, A. Haapalinna, P. Kärhä, and E. Ikonen, Non-linearity measurements of silicon photodetectors, Appl. Opt., 1998, 37: 2716-2722.

[13] H. Yamagishi, Y. Suzuki, and A. Hiraide, Precise Measurement of Photodiode Spectral Responses Using the Calorimetric Method, IEEE Tran. Instrum. Meas. 1989, 38: 578-580.

[14] X. S. Meng, Y. Huang, Z. H. He, Y. Q. Lin, S. D. Liu, D. C. Li, J. Li, X. Y. Qiu, Circularly polarized light to study linear magneto-optics for ferrofluids: θ-scan technique, Measur. Sci. Tech., 2018, 29: 065202 (8pp).

[15] X. S. Meng, J. Li, Y. Q. Lin, X. D. Liu, N. N. Liu, W. J. Ye, D. C. Li, Z. H. He, Polymer dispersed liquid crystals doped with low concentration γ-Fe_2O_3 nanoparticles, Liq. Cryst., 2021, 48: 1791-1805.

[16] V. Socoliuc, L. B. Popescu, Extinction of polarized light in ferrofluids with different particle concentrations, J. Magn. Magn. Mater., 2012, 324: 113-123.

[17] F. Bloisi, L. Vicari, Laser beam manipulation by composite material electro-optic devices, Opt. Lasers Eng., 2003, 39: 389-408.

[18] G. B. Hadjichristov, Y. G. Marinov, A. G. Petrov, Gradient polymer-dispersed liquid crystal single layer of large nematic droplets for modulation of laser light, Appl. Opt., 2011, 50: 2326-2333.

[19] J. W. Doane, A. Golemue, J. L. West, J. B. Whitechead Jr., and B. –G. Wu, Polymer Dispersed Liquid Crystals for Display Application, Mol. Cryst. Liq. Cryst., 1988, 165: 511-532.

[20] P. Mormile, L. Petti, M. Abbate, P. Musto, G. Ragosta, P. Villano, Temperature switch and thermally induced optical bistability in a PDLC, Opt. Commum., 1998, 147:269-273.

[21] R. Fernández, S. Gallego, A. Márquez, J. Francés, V. N. Fuster, C. Neipp, M. Qrtuňo, A. Beléndez, I. Pascual, Shrinkage measurement for holographic recording materials, Proc. of SPIE, 2017, 10233: 102330C (9pp).

[22] A. Kumari & A. Sinha, Role of $BaTiO_3$ nanoparticles on electro-optic performance of epoxy-resin-based PDLC devices, Liq. Cryst., 2021, 48: 23-34.

Figure caption

Fig.1 Measurement configuration of the power by the light power meter and voltage by the Si photodiode detector. (1) He-Ne laser, (2) polarizer, (3) quarter-wave plate, (4) polarizer, (5) analyzer and rotating stage, (6) photoelectric sensors (PD300R-UV), (7) light power meter (StarLite), (8) Si photodiode detector (7ID230), (9) data acquisition board, (10) computer in LabVIEW environment.

Fig.2 Measurement configuration of electro-optical effects for the PDLC. (1) He-Ne laser, (2) attenuator, (3) polarizer, (4) quarter-wave plate, (5) polarizer, (6) spectroscope, (7) diaphragm, (8) PDLC film, (9) diaphragm, (10) Si photodiode detector (7ID230), (11) Si photodiode detector (7ID230), (12) photodiode sensor (PD300R-UV), (13) light power meter (StarLite), (14) data acquisition board, (15) voltage amplifier, (16) computer in LabVIEW environment.

Fig.3 The P-θ curve and V-θ curve were measured by the light power meter and photodiode detectors. (a) the P-θ curve, (b) the V-θ curve

Fig.4 The comparison of the measured V-P and fitted curves.

Fig.5 The T-V curves of the PDLC film were measured by the Si photodiode detectors and light power meter, respectively. (a) the T^{V}-V_{appl} curves of the PDLC measured by the Si photodiode detectors, (b) T^{P}-V_{appl} curves of PDLC measured by the light power meter.

Fig.6 The T^{P}-V_{appl} curves measured by the light power meter, and the corrected curves $T^{V,c}$-V_{appl} measured by the Si photodiode detectors with different incident light power. (a) the incident light power is 1.1 μW, (b) the incident light power is 110 μW, (c) the incident light power is 1100 μW.

Fig.7 The response curves of the PDLC film were measured by the Si photodiode detector and light power meter, respectively.

Table caption

Tab.1 When the incident light power is 1.1, 110, and 1100 μW, the electro-optical parameters of PDLC film measured by the Si photodiode detectors and light power meter, respectively.

Fig.1

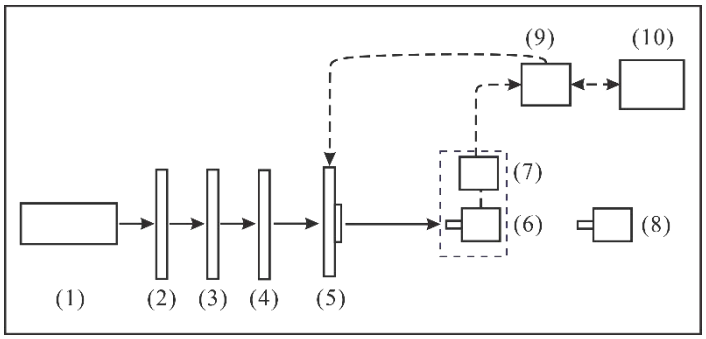

Fig.2

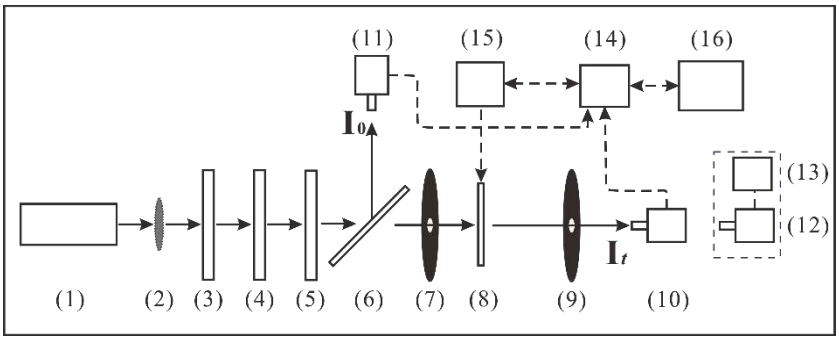

Fig.3

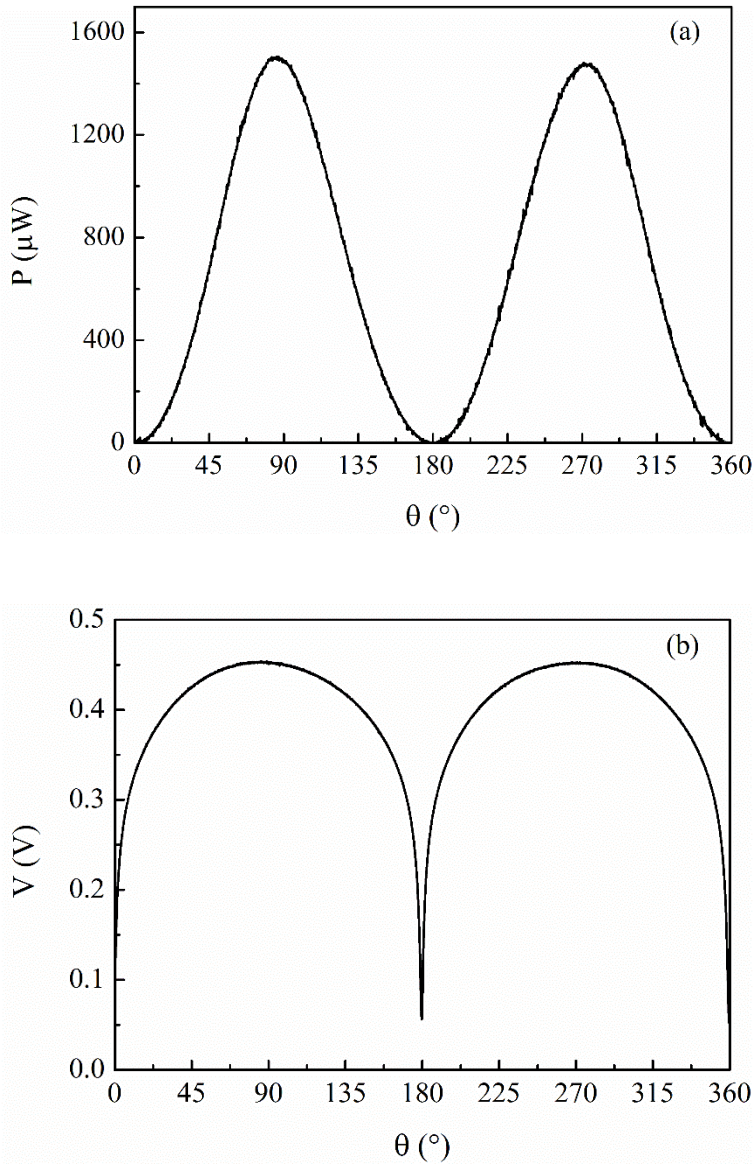
(a)
P (μW)
1600
1200
800
400
0
0
45
90
135
180
225
270
315
360
θ (°)
(b)
V (V)
0.5
0.4
0.3
0.2
0.1
0.0
0
45
90
135
180
225
270
315
360
θ (°)

Fig.4

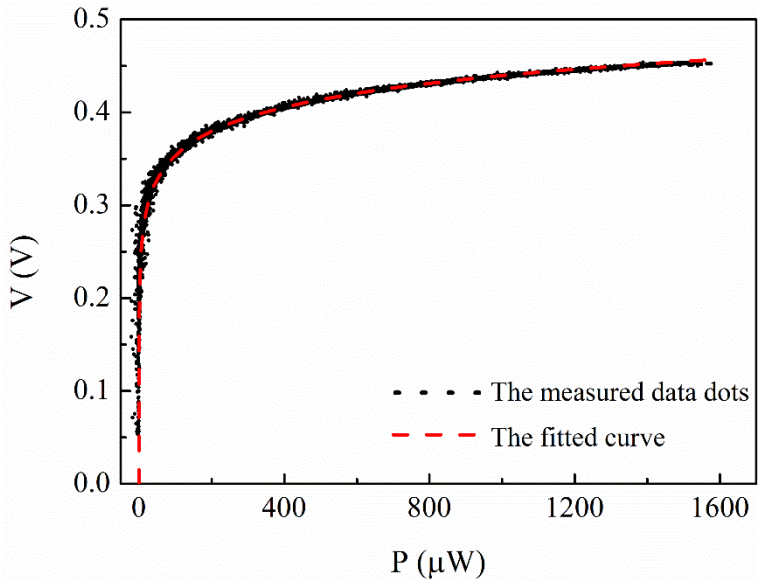
0.5
0.4
0.3
0.2
0.1
0.0
V (V)
0
400
800
1200
1600
P (μW)
The measured data dots
The fitted curve

Fig.5

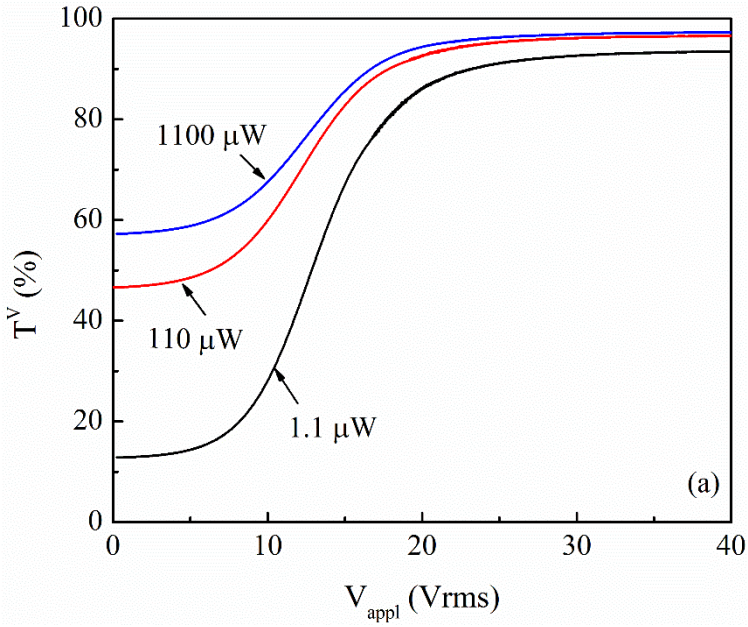
100
80
60
40
20
0
0
10
20
30
40
1100 μW
110 μW
1.1 μW
(a)
T^V (%)
V_{appl} (Vrms)

(a)

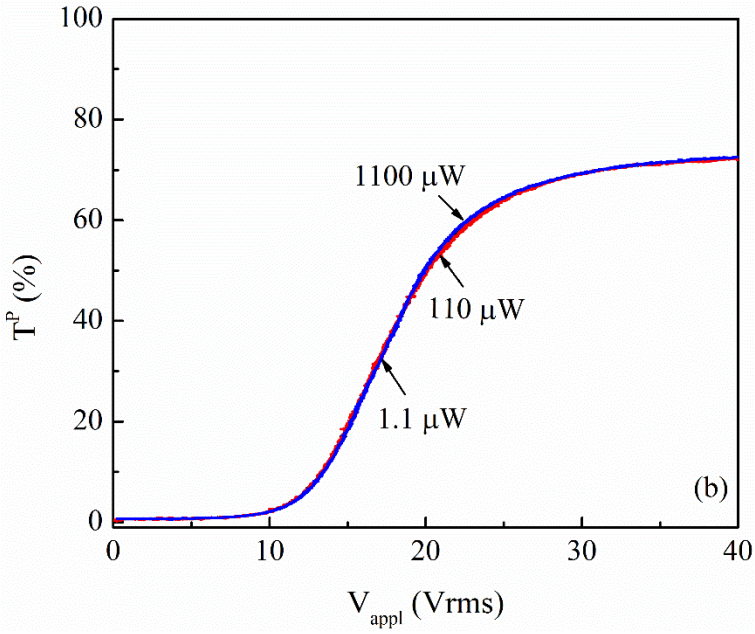
100
80
60
40
20
0
0
10
20
30
40
1100 μW
110 μW
1.1 μW
(b)
T^P (%)
V_{appl} (Vrms)

(b)

Fig.6

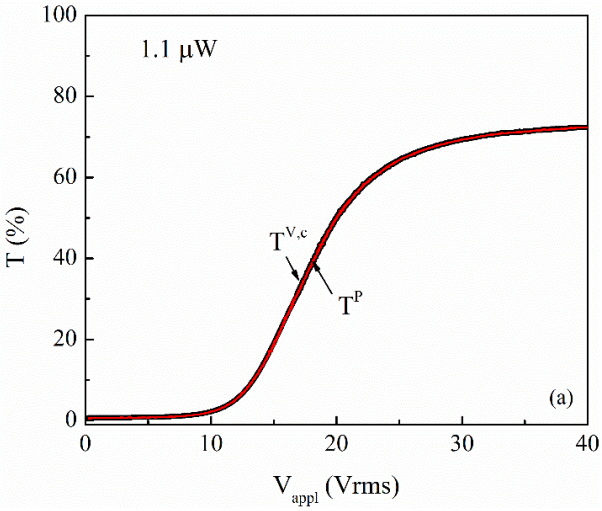
1.1 μW
T (%)
$T^{V,c}$
T^{P}
(a)
V_{appl} (Vrms)

(a)

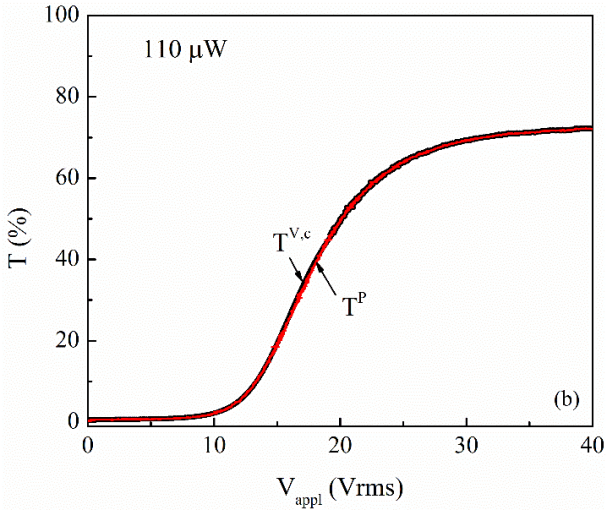
110 μW
T (%)
$T^{V,c}$
T^{P}
(b)
V_{appl} (Vrms)

(b)

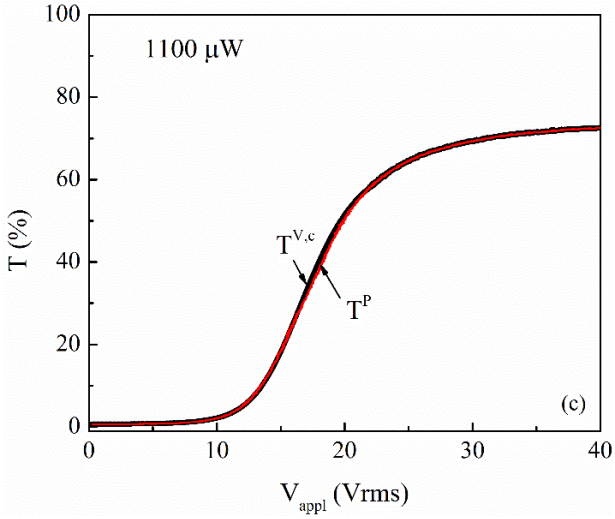
1100 μW
T (%)
$T^{V,c}$
T^{P}
(c)
V_{appl} (Vrms)

(c)

Fig.7

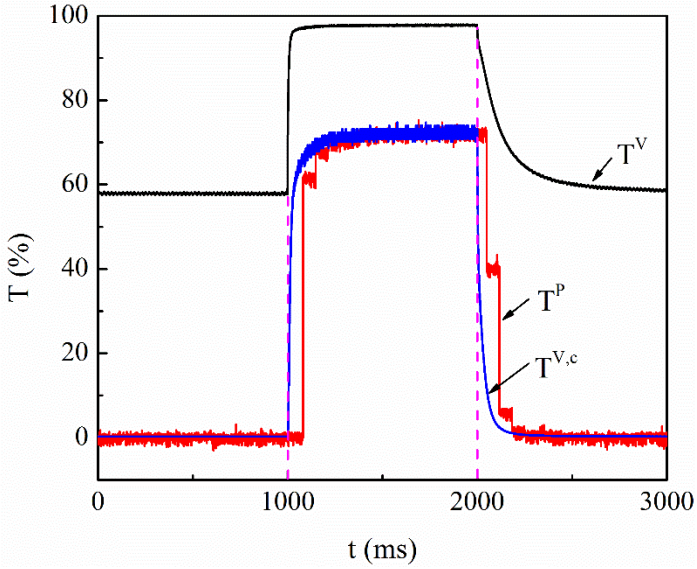

Tab.1

	SPD			LPM		
	1.1	110	1100	1.1	110	1100
$\boldsymbol{T}_0$ (%)	12.90	46.49	57.26	0.66	0.66	0.66
$\boldsymbol{T}_{sat}$ (%)	93.55	96.50	97.54	72.34	72.17	72.37
$\boldsymbol{V}_{th}$ (Vrms)				12.69	12.65	12.78
$\boldsymbol{V}_{sat}$ (Vrms)	19.11	16.30	15.66	25.50	25.60	25.35